A Multi-Parametric Diffusion Magnetic Resonance Imaging Texture Feature Model for Prostate Cancer Analysis

Farzad Khalvati, Amen Modhafar, Andrew Cameron, Alexander Wong, and Masoom A. Haider

Abstract In this work, we present a new multi-parametric magnetic resonance imaging (MP-MRI) texture feature model for automatic detection of prostate cancer. In addition to commonly used imaging sequences in conventional MP-MRI, namely T2-weighted MRI (T2w) and diffusion-weighted imaging (DWI), our proposed MP-MRI texture feature model uses computed high-b DWI (CHB-DWI) and a new diffusion imaging sequence called correlated diffusion imaging (CDI). A set of texture features was calculated for both the conventional MP-MRI and new MP-MRI texture feature model. We evaluated the performance of the proposed MP-MRI texture feature model via leave-one-patient-out cross-validation using a Bayesian classifier trained on cancerous and healthy tissue samples obtained from real clinical MP-MRI datasets. The proposed MP-MRI texture feature model outperformed the conventional model (i.e., T2w+DWI) with regard to cancer detection accuracy.

1 Introduction

Prostate cancer is the most common form of cancer and second leading cause of cancer death diagnosed in North American men, with more than 262,000 new cases and an estimated 33,660 deaths in 2013 [1,2]. Given that the median patient survival time for metastatic prostate cancer ranges from 12.2 to 21.7 months [3], early diagnosis of clinically significant prostate cancer would have significant benefits to patient care. This is particularly true given that the 5 year survival rate after diagnosis for patients with prostate cancer at the non-metastatic stage is 96 % in Canada [4].

F. Khalvati (✉) • A. Modhafar • M.A. Haider
Sunnybrook Research Institute, Toronto, ON, Canada
e-mail: farzad.khalvati@sri.utoronto.ca

A. Cameron • A. Wong
University of Waterloo, Waterloo, ON, Canada
e-mail: a28wong@uwaterloo.ca

L. O'Donnell et al. (eds.), *Computational Diffusion MRI*, Mathematics and Visualization, DOI 10.1007/978-3-319-11182-7_8

In the current clinical model, men with positive digital rectal exam (DRE) and elevated prostate-specific antigen (PSA) require multicore random biopsies for risk stratification. However, there is an ongoing controversy about the role of prostate PSA as a screening test in prostate cancer. Two recent major randomized clinical trials [5, 6] have demonstrated that PSA screening contains a significant risk of overdiagnosis for prostate cancer where it is estimated that 50 % of screened men are diagnosed with prostate cancer. This leads to painful needle biopsies and subsequent potential overtreatment [5, 6]. Moreover, it has become increasingly clear that prostate biopsies are harmful as they cause discomfort and possible sexual dysfunction and may result in increased hospital admission rates due to infectious complications [7]. Nevertheless, PSA testing has proven to reduce prostate cancer mortality by 20–30 % at long-term follow-ups [8]. Therefore, the PSA testing remains an important biomarker in diagnosing prostate cancers that are clinically significant. The remaining challenge is how to improve the prostate cancer diagnosis to reduce the overdiagnosis of clinically insignificant cancers.

Automatic detection of prostate cancer as part of a clinical decision support system can potentially help radiologists in interpreting images more accurately. Specifically, multi-parametric MR imaging (MP-MRI) which combines T2-weighted MRI (T2w), diffusion-weighted imaging (DWI), and dynamic contrast enhanced imaging (DCE) has been found to be a promising method for prostate cancer diagnosis and it has been used in different prostate cancer detection algorithms. By taking advantage of the unique information provided by each individual imaging technique, MP-MRI can exploit the different characteristics of prostate tissue to improve differentiation between cancerous and surrounding tissues. For example, cancerous tissue in the prostate gland may exhibit a moderate drop in signal in T2w [9] (which characterizes differences in transverse (spin-spin) relaxation time of tissue); restricted diffusion in DWI [9] (which characterizes diffusion of water in tissue); earlier onset time, higher peak, and shorter peak time in DCE [10] (which characterizes the concentration of an injected gadolinium contrast agent over time as it passes into the extracellular extravascular space of the tissue). Although DCE is considered as part of MP-MRI, T2w+DWI is the most common MP-MRI because it does not require invasive contrast agent as DCE does.

Radiologists' interpretations of MP-MRI have shown to achieve good prostate cancer detection rates, reaching accuracies of 80 % in the peripheral zone of the prostate gland. Similarly, several algorithms have been proposed for auto-detection of prostate cancer using MP-MRI setting [11–14]. These algorithms usually compute a set of low-level features from the MP-MRI data to construct feature vectors. Next, a supervised classifier is trained using the computed feature vectors from the training cases and their associated 'ground-truth' labels (e.g., labeled healthy or cancerous). Finally, the trained classifier is used to classify new cases. The reported values for accuracy of cancerous versus healthy tissue classification ranges from 64 to 89 %, depending on the feature sets and training/test data.

The underlying challenge in all these auto-detection algorithms is whether there is enough separability between the cancerous and healthy tissues in the feature

space. This means if the separability is poor, even sophisticated feature extraction algorithms may not have a significant effect on the accuracy of cancer detection. On the other hand, improving the separability of cancerous and healthy tissues in the images would have a significant impact on the performance of cancer auto-detection algorithms, potentially reducing the dependency on the feature extraction methods.

In this paper, we propose a new MP-MRI texture feature model that, in addition to T2w and conventional DWI, uses computed high-b diffusion-weighted imaging (CHB-DWI) [15] and the recently proposed correlated diffusion imaging (CDI) [16]. Compared to DWI, CHB-DWI and CDI have both shown initial promise to improve visual separability of cancerous and healthy tissues in prostate, which can lead to improved performance of the proposed MP-MRI texture feature model for detecting prostate cancer. To the authors' best knowledge, the proposed texture feature model is the first that utilizes all of the above-mentioned MP-MRI modalities.

This paper is organized as follows: in Sect. 2, the proposed MP-MRI texture feature model is presented. Section 3 presents the testing methodology which includes the description of image data and the evaluation metrics used in this research. Sections 4 and 5 present the experimental results and conclusions, respectively.

2 Proposed Multi-Parametric Magnetic Resonance Imaging Texture Feature Model

In this section, we present the proposed MP-MRI texture feature model for prostate cancer and discuss the imaging and feature extraction methods used in the model.

2.1 Imaging Methods

This subsection summarizes the imaging methods used in the proposed MP-MRI feature model.

2.1.1 T2-Weighted Imaging

T2w is a MR imaging modality in which the sensitivity of tissue is characterized by measuring the relaxation time (spin-spin) of the applied magnetic field. The T2w imaging of the prostate usually shows a small reduction in signal in the cancerous tissue [9].

2.1.2 Diffusion-Weighted Imaging

DWI is a promising imaging modality in which the sensitivity of tissue to Brownian motion of water molecules is measured by applying pairs of opposing magnetic field gradient pulses [17]. The diffusion-weighted signal, S is measured as:

$$S = S_0 e^{-bD} \tag{1}$$

where S_0 is the signal intensity without the diffusion weighting, b consists of amplitude and duration of the diffusion pulses, and the time between the two pulses as well as the gyromagnetic ratio, and D represents the strength of the diffusion. The diffusion-weighted image (S) is usually generated with different b values which can be used to estimate D in Eq. 1, called apparent diffusion coefficient map (ADC), using least-squares or maximum likelihood strategies [18]. The cancerous tissue in ADC is usually represented by a darker intensity compared to the surrounding tissue.

2.1.3 Computed High-b Diffusion-Weighted Imaging (CHB-DWI)

Previous research has shown that high b-value DWI images (e.g., b-values greater than 1,000 s/mm^2) allow for increased delineation between tumours and healthy tissues [15, 19] which makes the prostate cancer detection more robust. Nevertheless, due to hardware limitations, most MRI machines in practice do not produce DWI with b-values higher than 1,500 s/mm^2. CHB-DWI is an alternative approach to obtain high-b DWI in which a computational model is used to reconstruct DWI at high b-values using low b-value DWI acquisitions [15]. For our experiments, we constructed CHB-DWI with b-value at 2,000 s/mm^2 using the same least squares estimation technique used for ADC, extrapolating to the b-value of 2000 s/mm^2.

2.1.4 Correlated Diffusion Imaging (CDI)

CDI [16] is a new diffusion magnetic resonance imaging modality, which takes advantage of the joint correlation in signal attenuation across multiple gradient pulse strengths and timings to not only reduce the dependency on the way diffusion gradient pulses are applied, but also improve delineation between cancerous and healthy tissue. The local correlation of signal attenuation across all b-values within a local sub-volume is calculated to better represent the overall characterization of the water diffusion properties of the tissue. The CDI signal is calculated as follows [16]:

$$\begin{aligned} CDI(x) = \int \dots \int_{b_0}^{b_n} & S_0(x) \dots S_n(x) P(S_0(x), \dots, S_n(x) | V(x)) \\ & \times dS_0(x) \dots dS_n(x) \end{aligned} \tag{2}$$

where x denotes spatial location, S denotes the acquired signal, P denotes the conditional joint probability density function, and $V(x)$ denotes the local subvolume around x.

2.2 Texture Feature Model

In order to separate the cancerous tissue from the healthy one, a set of features is calculated on a given MR imaging sequence (i.e., T2w, DWI, CHB-DWI, CDI). As part of the proposed MP-MRI texture feature model, we incorporate the texture features used in separate studies to establish a relationship between these features and tumour glucose metabolism and stage [20] and to predict the response of metastatic renal cell cancer to treatment [21]. These features include mean grey-level intensity (M), entropy (En), and uniformity (U), which are calculated as follows:

$$M = \frac{1}{N} \sum_{x,y=0}^{N-1} pix(i, j) \tag{3}$$

$$En = -\sum_{l=1}^{k} p(l) log_2[p(l)] \tag{4}$$

$$U = \sum_{l=1}^{k} [p(l)]^2 \tag{5}$$

where $pix(i, j)$ is the gray-level intensity in the pixel window, N is the window size, p is the probability density function of pixels in the window, and k is the number of grey levels in the image.

In addition, the proposed MP-MRI texture feature model incorporates another set of texture features extracted from the gray-level co-occurrence matrix (GLCM) in 4 directions: 0°, 45°, 90°, and 135°. The GLCM texture features are calculated as follows:

1. Contrast (Con)—a measure of the intensity difference between a pixel and its neighbors:

$$Con = \sum_{x,y=0}^{N-1} |x - y|^2 p_{glcm}(x, y) \tag{6}$$

2. Energy (Eg)—the sum of squared elements in the GLCM;

$$Eg = \sum_{x,y=0}^{N-1} p_{glcm}(x, y)^2 \tag{7}$$

3. Homogeneity (H)—a value that measures the closeness of the distribution of elements in the GLCM to the GLCM diagonal.

$$H = \sum_{x,y=0}^{N-1} \frac{p_{glcm}(x, y)}{1 + (x - y)^2} \tag{8}$$

4. Correlation (Cor)—a measure of how correlated a pixel is to its neighbors:

$$Cor = \sum_{x,y=0}^{N-1} \frac{(x - \mu_x)(y - \mu_y) p_{glcm}(x, y)}{\sigma_x \sigma_y} \tag{9}$$

where p_{glcm} is the probability value from the GLCM, μ_x, μ_y, σ_x, and σ_y are the means and standard deviation values of p_{glcm} in horizontal and vertical directions, respectively.

As a result, the proposed MP-MRI texture feature model consists of a total of 19 features for each imaging modality: 16 from GLCM (4 in each direction) and 3 other texture features (i.e., mean gray level, entropy, and uniformity).

3 Testing Methodology

In the following, details about the image acquisition protocols and the performance measures are presented.

3.1 Image Data

MRI data of five patients were acquired using a Philips Achieva 3.0T machine at Sunnybrook Health Sciences Centre, Toronto, Ontario, Canada. All data was obtained under the local institutional research ethics board. For each patient, the following MP-MRI modalities were obtained (Table 1): T2w, DWI, and CDI. The patients' age ranged from 53 to 75.

Table 1 Description of the prostate T2w, DWI, and CDI images

Sequence	DFOV (cm^2)	Resolution (mm^2)	Resolution (pixels)	TE (ms)	TR (ms)
T2w	22 × 22	0.49 × 0.49 × 3	440 × 425 × 26	110	4,687
DWI	20 × 20	1.56 × 1.56 × 3	128 × 128 × 24	61	6,178
CDI	20 × 20	1.56 × 1.56 × 3	128 × 128 × 24	61	6,178

3.2 Evaluation Metrics

We evaluated the performance of the proposed MP-MRI texture feature model for detecting prostate cancer via a leave-one-patient-out cross-validation using a Bayesian classifier. First, the feature extraction function was applied to each MR imaging sequence (i.e., T2w, ADC, CHB-DWI, and CDI) separately across all patients' data. This generated four sets of features based on the proposed MP-MRI texture feature model. Next, a conventional MP-MRI setting was established by combining the features of T2w and ADC. As a new MP-MRI texture feature model, three configurations were realized: T2w+ADC+CHB-DWI, T2w+ADC+CDI, and CHB-DWI+ADC+CDI.

We used a Bayesian classifier to calculate sensitivity, specificity, and accuracy using leave-one-patient-out cross-validation approach. As ground-truth, all images were reviewed and marked as healthy and cancerous tissue by a radiologist with 18 and 13 years of experience interpreting body and prostate MRI, respectively.

4 Experimental Results

Table 2 shows sensitivity, specificity, and accuracy for all 8 MP-MRI modalities/models. For each modality, on average, 5,260 (5,110 healthy and 150 cancerous) and 1,315 (1,275 healthy and 40 cancerous) samples (i.e., pixel windows) were used as training and testing data, respectively for the leave-one-patient-out cross-validation. The results were averaged across all patients. In order to unify all three measures (sensitivity, specificity, and accuracy) for the purpose of comparison among different configurations, we also report the average of the three measures for each modality/configuration.

It is seen that CHB-DWI alone improves results compared to T2w and ADC (Sensitivity: 0.88 vs. 0.70 and 0.87, Specificity: 0.58 vs. 0.48 and 0.37, Accuracy: 0.58 vs. 0.49 and 0.38). Although CDI has a lower sensitivity compared to T2w (0.66 vs. 0.70), its specificity and accuracy is the highest among all individual

Table 2 Evaluation results for prostate cancer detection

Imaging modality	Sensitivity	Specificity	Accuracy	Average
T2w	0.7037	0.4815	0.4878	0.5577
ADC	0.8730	0.3659	0.3805	0.5398
CHB-DWI	0.8836	0.5751	0.5839	0.6809
CDI	0.6614	0.7998	0.7958	0.7523
T2w+ADC	0.8360	0.4096	0.4219	0.5558
T2w+ADC+CHB-DWI	0.8571	0.6350	0.6414	0.7112
T2w+ADC+CDI	0.6772	0.8125	0.8086	0.7661
CHB-DWI+ADC+CDI	0.7831	0.7867	0.7866	0.7854

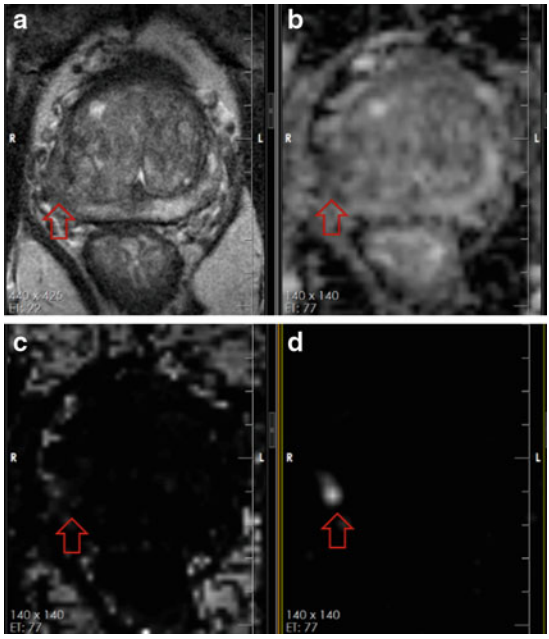

Fig. 1 (**a**) T2w does not clearly show a tumour although there is mild signal alteration in the left peripheral zone (*arrow*). (**b**) ADC does not clearly show a tumour (*arrow*). (**c**) CHB-DWI of 2,000 s/mm^2 shows no tumour (*arrow*). (**d**) CDI clearly shows a bright nodule (*arrow*) corresponding to tumour

modalities (0.80). This is due to the fact that CDI combines the information across b-values making it robust.

The first configuration of the new MP-MRI texture feature model, T2w+ADC+CHB-DWI, improves the results with regard to the conventional model, T2w+ADC, (Sensitivity: 0.86 vs. 0.84, Specificity: 0.63 vs. 0.41, Accuracy: 0.64 vs. 0.42). The second configuration of the new MP-MRI texture feature model, T2w+ADC+CDI, loses the sensitivity compared to the conventional model, T2w+ADC, (0.68 vs. 0.84) but outperforms it in both specificity (0.81 vs. 0.41) and overall accuracy (0.81 vs. 0.42). The third configuration of the proposed MP-MRI (CHB-DWI+ADC+CDI) only loses 5 % in sensitivity compared to the conventional MP-MRI (T2w+ADC) (0.783 vs 0.836). In return, it improves the specificity and accuracy by 38 and 37 %, respectively (Specificity: 0.79 vs. 0.41, Accuracy: 0.79 vs. 0.42). In other words, with a slight reduction in true positive cases, a significant amount of false positive cases can be avoided. The best result for average of all three measures (i.e., sensitivity, specificity, and produced by CHB-DWI+ADC+CDI (0.79).

Figure 1 shows an example for all four modalities which include T2w, ADC, CHB-DWI, and CDI. As it can be seen, CDI (Fig. 1d) is the only modality that clearly shows a bright nodule where a tumour is located (confirmed by histopathology data).

5 Conclusions

In this paper, we introduced a new multi-parametric MRI texture feature model for prostate cancer detection. Our new MP-MRI texture feature model adds two new image modalities, CHB-DWI and CDI, to the most commonly used MP-MRI, T2w+ADC. We calculated a set of texture features for both the conventional MP-MRI and new MP-MRI texture feature models. A Bayesian classifier was trained via leave-one-patient-out setting to classify the new cases. We evaluated the proposed MP-MRI texture feature model in three configurations. The first configuration (T2w+ADC+CHB-DWI) improved the results (sensitivity, specificity, and accuracy) compared to the conventional MP-MRI. The second configuration (T2w+ADC+CDI) improved specificity (40 %) and accuracy significantly (39 %) with a loss in sensitivity (16 %) with respect to the conventional MP-MRI. The best result was achieved by the third configuration (CHB-DWI+ADC+CDI); it improved specificity and accuracy significantly (38 and 37 %, respectively) with a rather small loss in sensitivity (5 %) with respect to the conventional MP-MRI. The proposed MP-MRI texture feature model showed promise to tackle the overdiagnosis problem in prostate cancer detection.

References

1. Canadian Cancer Society: Canadian Cancer Statistics (2013)
2. American Cancer Society: Cancer Facts and Figures (2013)
3. Ren, J., Wang, F., Wei, G., Yang, Y., Liu, Y., Wei, M., Huan, Y., Larson, A.C., Zhang, Z.: MRI of prostate cancer antigen expression for diagnosis and immunotherapy. PLoS ONE **7**(60), e38350 (2012)
4. Canadian Cancer Society: Canadian Cancer Statistics (2011)
5. Andriole, G.L., et al.: PLCO Project Team. Mortality results from a randomized prostate-cancer screening trial. N. Engl. J. Med. **360**, 1310–1319 (2009)
6. Schroder, F.H., et al.: ERSPC Investigators, screening and prostate-cancer mortality in a randomized European study. N. Engl. J. Med. **360**, 1320–1328 (2009)
7. Loeb, S., et al.: Systematic review of complications of prostate biopsy. Eur. Urol. **64**(6), 876–892 (2013)
8. Schroder, F.H., et al.: ERSPC Investigators. Prostate-cancer mortality at 11 years of follow-up. N. Engl. J. Med. **366**(11), 981–990 (2012)
9. Haider, M.A., van der Kwast, T.H., Tanguay, J., Evans, A.J., Hashmi, A.T., Lockwood, G., Trachtenberg, J.: Combined T2-weighted and diffusion-weighted MRI for localization of prostate cancer. AJR. Am. J. Roentgenol. 189(2), 323–328 (2007)
10. Langer, D.L., van der Kwast, T.H., Evans, A.J., Plotkin, A., Trachtenberg, J., Wilson, B.C., Haider, M.H.: Prostate tissue composition and MR measurements: investigating the relationships between ADC, T2, K-trans, v(e), and corresponding histologic features. Radiology **255**(2), 485–494 (2010)
11. Ozer, S., Haider, M.A., Langer, D.L., van der Kwast, T.H., Evans, A.J., Wernick, M.N., Trachtenberg, J., Yetik, I.S.: Prostate cancer localization with multispectral MRI based on relevance vector machines. In: 2009 IEEE International Symposium on Biomedical Imaging From Nano to Macro, IEEE, pp. 73–76 (2009)

12. Madabhushi, A., Feldman, M.D., Metaxas, D.N., Tomaszeweski, J., Chute, D.: Automated detection of prostatic adenocarcinoma from high-resolution ex vivo MRI. IEEE Trans. Med. Imaging **24**(12), 1611–1625 (2005)
13. Liu, X., Langer, D.L., Haider, M.A., Yang, Y., Wernick, M.N., Yetik, I.S.: Prostate cancer segmentation with simultaneous estimation of Markov random field parameters and class. IEEE Trans. Med. Imaging **28**(6), 906–915 (2009)
14. Ozer, S., Langer, D.L., Liu, X., Haider, M.A., van der Kwast, T.H., Evans, A.J., Yang, Y., Wernick, M.N., Miles, N., Yetik, I.S.: Supervised and unsupervised methods for prostate cancer segmentation with multispectral MRI. Med. Phys. **37**(4), 1873–1883 (2010)
15. Glaister, J., Cameron, A., Wong, A., Haider, M.A.: Quantitative investigative analysis of tumour separability in the prostate gland using ultra-high b-value computed diffusion imaging. In: EMBC'2012, IEEE pp. 420–423 (2012)
16. Wong, A., Glaister, J., Cameron, A., Haider, M.A.: Correlated diffusion imaging. BMC Med. Imaging **13**, 26 (2013)
17. Koh, D.M., Padhani, A.R.: Diffusion-weighted MRI: a new functional clinical technique for tumour imaging. Br. J. Radiol. **79**, 633–635 (2006)
18. Walker-Samuel, S., Orton, M., McPhail, L.D., Robinson, S.P.: Robust estimation of the apparent diffusion coefficient (ADC) in heterogeneous solid tumors. Magn. Reson. Med. **62**(2), 420–429 (2009)
19. Rosenkrantz, A.B., Chandarana, H., Hindman, N., Deng, F.M., Babb, J.S., Taneja, S.S., Geppert, C.: Computed diffusion-weighted imaging of the prostate at 3T: impact on image quality and tumor detection. Proc. Int. Soc. Magn. Reson. Med. **21**, 94 (2013)
20. Ganeshana, B., Abaleke, S., Young, R.C., Chatwin, C.R., Miles, K.A.: Texture analysis of non-small cell lung cancer on unenhanced computed tomography: initial evidence for a relationship with tumour glucose metabolism and stage. Cancer Imaging **10**, 137–143 (2010)
21. Goh, V., Ganeshan, B., Nathan, P., Juttla, J.K., Vinayan, A., Miles, K.A.: Assessment of response to tyrosine kinase inhibitors in metastatic renal cell cancer: CT texture as a predictive biomarker. Radiology **261**(1), 165–71 (2011)